remote sensing

MDPI

Article

Evaluating the Effects of Wetland Restoration on Ecosystem Services Using InVEST and Geostatistics: A Case Study of Dongting Lake in China

Jiaying Zhou [1,2], Zijian Wang [1,2], Ying He [1,2], Peizhong Liu [1,2], Jie Xu [2], Cai Lu [1,2], Guangchun Lei [1,2] and Li Wen [1,3,*]

[1] Centre for East Asian-Australasian Flyway Studies, Beijing Forestry University, Beijing 100083, China; luluzhou@bjfu.edu.cn (J.Z.); zjwang@bjfu.edu.cn (Z.W.); abbyisxyz33@bjfu.edu.cn (Y.H.); peizhongliu@bjfu.edu.cn (P.L.); cailu@bjfu.edu.cn (C.L.); leiguangchun@bjfu.edu.cn (G.L.)
[2] School of Ecology and Nature Conservation, Beijing Forestry University, Beijing 100083, China; jiexu@bjfu.edu.cn
[3] Science and Insights Division, NSW Department of Climate Change, Energy, the Environment and Water, Parramatta, NSW 2150, Australia
* Correspondence: li.wen@environment.nsw.gov.au

Abstract: Ecological restoration projects aim to recover ecosystems that have been degraded, damaged, or destroyed. The effective assessment of these projects is crucial for ensuring that restoration goals are met and for guiding future efforts. The Poplar Ecological Restoration Project (PERP), focused on removing floodplain poplar plantations, is a key environmental initiative in China to preserve the ecological functions and services of the Dongting Lake freshwater wetland complex. Understanding the dynamic changes in ecosystem services and their trade-offs/synergies before and after the project is crucial for ensuring that ecosystem services are maintained and enhanced. This study selected three key ecosystem services, water conservation, carbon storage, and habitat quality, as indicators to assess the PERP. Using the Integrated Valuation of Ecosystem Services and Trade-offs (InVEST) model and geostatistical methods, including the Spearman correlation analysis and spatial autocorrelation analysis, we explored the ecological outcomes of the project. The results indicated that since its implementation in 2014, the PERP has significantly altered the land use and land cover (LULC) in the lake. Most of the former plantations have been converted into reedbeds (17,404 ha), followed by sedgelands (3841 ha), mudflats (443 ha), shallow waters (382 ha), and deep waters (301 ha). During this period, water conservation and habitat quality initially decreased and then increased, while carbon storage continuously declined. Overall, all assessed services showed an increasing trend except for carbon storage, resulting in a slight decrease in the integrated ecosystem services. Moreover, there were strong bivariate associations among the three investigated ecosystem services, and the synergies were strengthened during the project. Importantly, these synergies became positive after the PERP, meaning that the improvement of one service enhanced others, potentially leading to a more sustainable and resilient ecosystem.

Keywords: ecological restoration; ecosystem services; synergies/trade-offs; InVEST; Dongting Lake

check for updates

Citation: Zhou, J.; Wang, Z.; He, Y.; Liu, P.; Xu, J.; Lu, C.; Lei, G.; Wen, L. Evaluating the Effects of Wetland Restoration on Ecosystem Services Using InVEST and Geostatistics: A Case Study of Dongting Lake in China. *Remote Sens.* **2024**, *16*, 4062. https://doi.org/10.3390/rs16214062

Academic Editor: Melanie Vanderhoof

Received: 23 August 2024
Revised: 17 October 2024
Accepted: 28 October 2024
Published: 31 October 2024

Copyright: © 2024 by the authors. Licensee MDPI, Basel, Switzerland. This article is an open access article distributed under the terms and conditions of the Creative Commons Attribution (CC BY) license (https://creativecommons.org/licenses/by/4.0/).

1. Introduction

Wetlands are vital ecosystems that provide numerous ecological, economic, and social benefits [1]. They act as natural water filters, help in flood control, support biodiversity by providing habitat for various species, and play a significant role in carbon sequestration [2]. Despite their importance, wetlands are under continuous threat from human activities such as agriculture, urban development, and pollution [3], leading to significant wetland loss and degradation. For example, 53–62% of wetlands in the United States were lost in the past 100–200 years [4]. In England, over the past 500 years, approximately 90% of its wetlands

have been lost [5]. In China, 60% of its natural coastal wetlands have been lost to economic development since the 1950s [6]. Therefore, effective conservation strategies are essential to protect these valuable ecosystems and ensure their sustainability for future generations.

Wetland restoration is a global environmental initiative in contemporary environmental management [7,8] that aims to rehabilitate these damaged ecosystems by reestablishing their natural processes, hydrology, and vegetation, thereby enhancing habitat quality and ecosystem services (ESSs). Monitoring and assessing ecological restoration projects are vital components for ensuring the success and sustainability of these initiatives [9], providing critical feedback that informs ongoing and future restoration activities, and ensuring that they are based on sound scientific principles and that they achieve desired ecological outcomes.

The assessment of wetland restoration projects, however, has evolved to include not just biophysical and ecological parameters, but also the outcomes of ESSs they deliver. ESSs are the benefits that humans derive from ecosystems. These can be categorized into four main types: provisioning services (such as food and water), regulating services (such as climate regulation and flood control), supporting services (such as nutrient cycling and soil formation), and cultural services (such as recreational and spiritual benefits).

The InVEST (Integrated Valuation of Ecosystem Services and Trade-offs) model is a suite of tools developed by the Natural Capital Project to quantify the value of ESSs and understand how different management strategies impact these services [10,11]. This model enables the assessment of changes in ESSs before and after restoration, providing a clear picture of the benefits achieved through restoration efforts. It can also identify trade-offs and synergies between different services, helping to optimize restoration strategies for multiple ecological and socio-economic objectives. Applied to wetlands, the InVEST model can evaluate critical services such as water purification, carbon sequestration, and habitat provision by integrating ecological, hydrological, and socio-economic data. However, most of the current applications of InVEST for wetland restoration evaluation are focused on a single dimension, such as providing suitable habitats to support biodiversity [12], and there is a lack of comprehensive analysis. Moreover, trade-off analyses between wetland ESSs are also sparse [13].

Dongting Lake, as a Ramsar international important wetland, holds a pivotal position in freshwater ecosystems in China and provides essential ESSs, such as the provision of a quality habitat for wintering migratory waterbirds [14,15]. Since the 1970s, the introduction of poplar (*Populus euramericana*), a species with strong adaptability and high economic benefits, has led to a rapid expansion of its plantation at the expense of other key areas essential for fish and waterbirds [16]. For example, from 1996 to 2013, the poplar plantation area in West Dongting Lake increased ninefold, becoming a dominant local landscape [17]. Studies have shown a decline in herbaceous plant species richness and bird populations under poplar forests in Dongting Lake. Additionally, due to the high evapotranspiration rate, extensive poplar plantation exacerbates wetland drought, alters soil physicochemical properties, and drives the wetland towards a terrestrial ecosystem, earning the nickname "wetland pumps" [18].

The Poplar Ecological Restoration Project (PERP), a major initiative for poplar deforestation in Dongting Lake, was launched in 2014 to restore wetland ecosystems and protect regional biodiversity, representing a key policy for regional wetland restoration [19]. In October 2017, the PERP began large-scale implementation, resulting in the felling of nearly three million poplars across more than 50,000 hectares by the end of the year. In the same year, all poplars were removed from the core area of the Dongting Lake Wetland Nature Reserve. From 2018 to 2020, the government introduced a three-year action plan for the special treatment of the Dongting Lake ecological environment, further expanding the PERP area to buffer and experimental zones [12]. By the end of 2020, 6.5 million poplars had been felled from 2000 km^2 [19]. This intervention has led to significant changes in wetland land cover and ecosystem structure and functions, such as biodiversity, habitat quality, and water vapor regulation.

Several studies have demonstrated the positive ecological outcomes of the PERP, such as enhanced water conservation [19], improved habitat quality for migratory waterbirds [12], and increased soil bacteria diversity and richness [20]. However, to the best of our knowledge, no research has systematically investigated the EES outcomes of the PERP while considering the trade-offs and synergies between multiple ESSs. This lack of comprehensive analysis hinders our understanding of the restoration's effectiveness, which is crucial for making informed decisions, optimizing restoration practices, and demonstrating the value of wetlands to policymakers and the public [21].

In this study, we employed the InVEST model to investigate the spatiotemporal evolution of three essential ecosystem services (EESs)—water conservation, carbon storage, and habitat provision—from 2014 to 2021 under the PERP. The reliable distribution of land use and land cover (LULC) is crucial for parameterizing InVEST [11]. However, LULC classification for wetlands is challenging due to their dynamic nature and the lack of standardized classification methods [22]. To address this, we accurately mapped the LULC changes in the PERP area by integrating vegetation phenology, remote sensing technology, and machine learning algorithms. Subsequently, we quantified the changes in the selected EES using InVEST, which provided quantitative and spatially explicit information on service provision. We also explored the trade-offs and synergies of the ESSs using geostatistical methods. This study serves as a case study for applying InVEST to evaluate a large-scale wetland restoration project comprehensively. It provides valuable insights and recommendations for both practitioners and researchers involved in wetland conservation.

2. Materials and Methods

2.1. Study Area

The Dongting Lake wetland ecosystem (111°42′44″–113°39′45″E, 28°39′20″–30°14′18″N, Figure 1) is situated in the floodplains of the Middle Yangtze River Basin, encompassing a natural wetland area of 2625 km^2 and a total reservoir capacity of 16.7 billion m^3 [23]. It is the second largest freshwater lake wetland ecosystems in China and a crucial wintering ground for migratory birds along the East Asia–Australasian Flyway [24]. The study area roughly includes the regions covered by the Poplar Ecological Restoration Project (PERP).

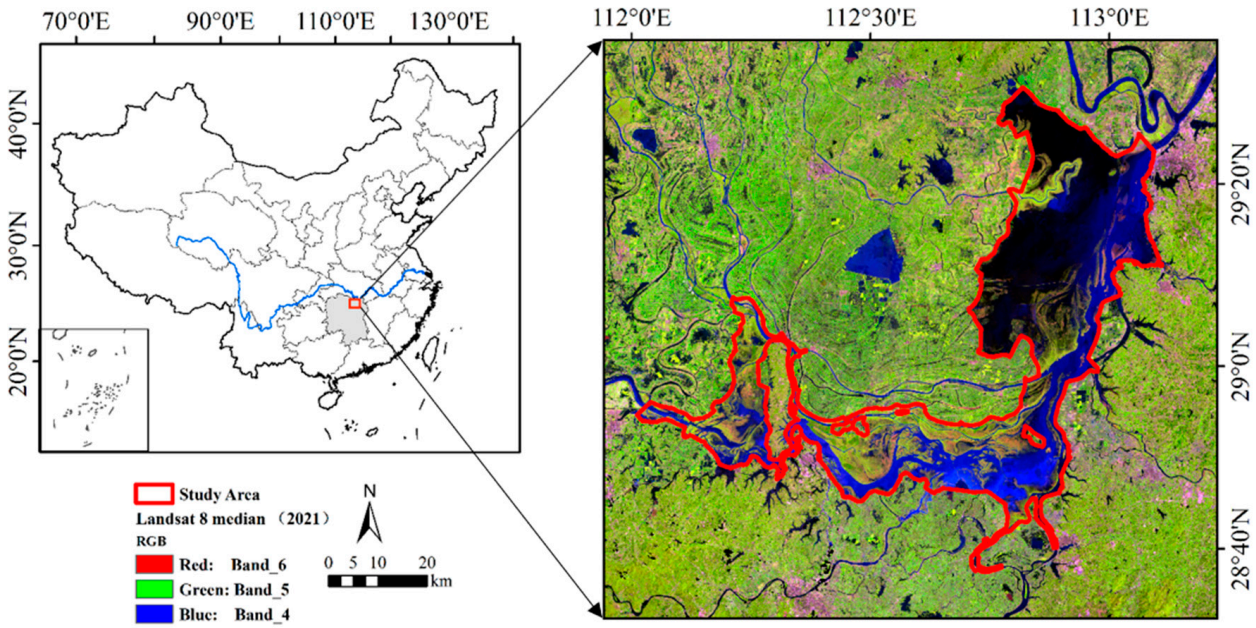


Figure 1. Study area of the Dongting Lake wetland complex in China; the background is the median Landsat 8 image in the summer of 2021. The inset map shows the location of Dongting Lake in China.

The region experiences a subtropical monsoon climate, characterized by warm and humid conditions. The annual average temperature ranges from 16.4 °C to 17 °C, with a frost-free period of 258 to 275 days. The annual average precipitation is between 1100 and 1400 mm, with uneven distribution concentrated mainly from April to June, during which heavy rains and storms are common, often leading to flooding [25].

2.2. Data Sources

Data from multiple sources were used for InVEST model parametrization (Table 1). The atmospherically corrected surface reflectance data (USGS Landsat 8 Level 2, Collection 2, Tier 1) were sourced from and preprocessed using the Google Earth Engine (GEE) cloud computing platform for LULC classification. Cloud-contaminated pixels were excluded using the QA_PIXEL band. The specific acquisition dates of the selected images are provided in Supplementary Table S1.

Table 1. Data used for InVEST model parameterization (all websites are accessible before 25 June 2024).

Data	Source	Type	Temporal Frequencies
Landsat 8-OLI	Google Earth Engine (http://earthengine.google.com/)	Grid	16-day
Precipitation and potential evapotranspiration	National Earth System Science Data Center (http://www.geodata.cn/)	Grid	monthly
Soil type and soil depth	Harmonized World Soil Database version 1.2 (https://data.tpdc.ac.cn/zh-hans/data/844010ba-d359-4020-bf76-2b58806f9205/)	Grid	1
Root depth and flow coefficient	Hu et al. [19] and InVEST model 3.14 manual (http://releases.naturalcapitalproject.org/invest-userguide/latest/en/index.html)	Grid	1
Plant available water content	Calculated based on the equation from Natural Resource Conservation Service (NRCS) (http://soils.usda.gov/)	Grid	1
Roads	OpenStreetMap (https://www.openhistoricalmap.org/)	Polygon	yearly
Impervious surfaces and cropland	Derived from the annual China Land Cover Dataset (CLCD) (http://doi.org/10.5281/zenodo.4417809/)	Grid	yearly
Digital elevation models (DEMs)	JAXA/ALOS/AW3D30/V3_2 from Google Earth Engine (http://earthengine.google.com/)	Grid	1

Threat sources in habitat quality (impervious surfaces, farmland) were derived from the CLCD (annual China Land Cover Dataset), while road data were sourced from the OpenStreetMap official website (accessed on 25 April 2024, http://www.openhistoricalmap.org/).

2.3. Wetland Classification

The wetlands of Dongting Lake in 2014, 2017, and 2021 were classified into six categories: shallow water (SW), deep water (DW), reedbeds (RBs), sedgelands (SLs), forests (FRs), and mudflats (MLs) (Table 2).

2.3.1. Training Samples

We collected a total of 2480 field samples for classification model development and validation. Sample points were determined based on a number of resources, including field surveys, historical research [26], high-resolution Google Earth images, and high-resolution Hunan Province Tianditu images (https://hunan.tianditu.gov.cn/TDTHN/portal/map/multidatemap.html, accessed on 25 April 2024).

2.3.2. Predictor Variables

Spectral Indices

Recent studies have shown that the application of remote sensing spectral indices can effectively enhance the accuracy of land cover type identification [27]. This study incorporated the following spectral indices: Normalized Difference Vegetation Index (NDVI) [28],

Modified Normalized Difference Water Index (MNDWI) [29], Green Normalized Difference Vegetation Index (GNDVI) [30], Bare Soil Index (BSI) [31], and Mixed Leaf Area Index (MixLAI) [32].

Statistical data (standard deviation, minimum value, maximum value) for each vegetation index were computed using the GEE platform based on their respective formulas. These indices were sequentially added to the original remote sensing images. The calculation formulas for each index are as follows:

$$NDVI = \frac{\rho_{NIR} - \rho_{RED}}{\rho_{NIR} + \rho_{RED}} \quad (1)$$

$$MNDWI = \frac{\rho_{GREEN} - \rho_{SWIR1}}{\rho_{GREEN} + \rho_{SWIR1}} \quad (2)$$

$$GNDVI = \frac{\rho_{NIR} - \rho_{GREEN}}{\rho_{NIR} + \rho_{GREEN}} \quad (3)$$

$$BSI = \frac{(\rho_{RED} + \rho_{SWIR}) - (\rho_{NIR} + \rho_{BLUE})}{(\rho_{RED} + \rho_{SWIR}) + (\rho_{NIR} + \rho_{BLUE})} \quad (4)$$

$$\text{MixLAI} = \frac{\rho_{NIR}/(\rho_{RED} + \rho_{SWIR1}) + \rho_{NIR}/(\rho_{RED} + \rho_{SWIR2})}{2} \quad (5)$$

where ρ_{SWIR1}, ρ_{SWIR2}, ρ_{NIR}, ρ_{RED}, ρ_{GREEN}, and ρ_{BLUE} are the surface reflectance values of the shortwave infrared 1, shortwave infrared 2, near-infrared, red, green, and blue bands, respectively.

Phenological Metrics

Studies have indicated that certain wetland types exhibit similar spectral and/or backscatter behaviors in Landsat optical data, leading to high confusion in their classification [33]. Moreover, due to the dynamic nature of wetlands, using multi-temporal images has been found to improve classification accuracy [34]. Analyzing vegetation index time series by extracting seasonal parameters, known as phenological metrics, enhances the identification and classification of wetland ecosystems [35].

This study utilized the CropPhenology package [36] in the R programming environment [37] to extract vegetation phenological metrics. The following eight phenological indicators were computed: start of season (SOS), length of season (LOS), position of peak value (POP), position of trough value (POT), mean growing season value (MGS), peak value (PEAK), mean autumn value (MAU), and rate of spring greenup (RSP). These indicators were integrated into the classification process to enhance the accuracy of wetland ecosystem mapping and analysis.

2.3.3. Random Forest Classification

Machine learning classification methods such as support vector machine (SVM), classification and regression trees (CART), and random forest (RF) algorithms have been widely applied in land cover mapping and crop type identification [38]. We used the relatively new and high-performance RF algorithm that is an ensemble machine learning technique [39,40]. Considering the seasonality of the Dongting Lake wetland, i.e., most of the study area is underwater in the high-water season, only low-water season (15 October to 15 April) images were used for classification. Visual interpretation was conducted using different band combinations, and spectral indices, phenological indicators, and DEM data were used to train the classifier using the 2480 sample points. These samples were divided into two groups, with 80% being used for model training and the remaining 20% being used for validation. Accuracy metrics such as user accuracy, producer accuracy, overall accuracy, and Kappa coefficient were computed using the confusion matrix method [14].

Table 2. Wetland types in Dongting Lake for habitat quality module in InVEST and their characteristics.

Type		Characteristics	Image Description
Shallow water (SW)	a.	Water depth is <60 cm, and SW is generally located in the middle of each lake pool [41].	The SW is presented in light blue, adjacent to the DW.
	b.	SW is rich in aquatic plants, plankton, benthic organisms, and fish resources, and large waders and swimming birds can perch in SW.	
Deep water (DW)	a.	During the dry season, the water depth is >60 cm.	The DW is generally deep blue, close to the center of the lake
	b.	DW is usually located in the central area of Dongting Lake or near the main waterway leading into the lake. Some diving ducks, such as the redhead duck (*Aythya ferina*), can find food here.	
Reedbeds (RBs)	a.	The lake is separated by rivers, and it is surrounded by withered plants, forming a good lake cover.	The RB appears as a light yellow color in RGB images, with a wide distribution range, often indicating artificial traces such as grid-like roads and channels.
	b.	There are few waterfowls distributed.	
	c.	It mainly consists of high grass marshes such as common reed and reed canary grass (*Phalaris arundinacea*).	
Sedgelands (SLs)	a.	The soil is saturated with water, but the exposure time is relatively short.	SL generally appears as varying shades of red in the Landsat band 543 combination. The texture is smooth and fine, with minimal signs of human intervention.
	b.	The vegetation mainly consists of moss and *Carex spp.*, with the abundant waterfowl including the swan goose (*Anser cygnoides*), white-fronted goose (*Anser albifrons*), and lesser white-fronted goose (*Anser erythropus*).	
Forests (FRs)	a.	The long exposure time allows for the rapid growth of perennial herbaceous plants, resulting in high vegetation coverage.	FB appears as a darker shade of red in the Landsat band 543 combination. The rows of artificially planted poplar trees are relatively regular and have distinct boundary contours.
	b.	With a high biomass and strong concealment ability.	
Mudflats (MLs)	a.	The sediment deposited during the dry season is generally not covered by vegetation and has different sizes of pebbles and sand on its surface.	ML is usually white or light gray, appearing as stripes or surrounding water bodies and occasionally forming patches in the Landsat band 543 combination. It is distributed around lake, river banks, and lakeside grasslands.
	b.	The lake's water level further decreases due to natural evaporation or artificial drainage, resulting in an abundance of submerged plants and benthic organisms covering the surface.	

2.4. Calculation of Ecosystem Services

This study selected three key ecosystem services—water conservation, carbon storage, and habitat quality—to evaluate ESS outcomes of the PERP in the Dongting Lake ecosystem. Various types of data were collected and quantified to parameterize the InVEST sub-models.

2.4.1. Water Conservation

The evaluation of the water conservation function is based on the water yield module of the InVEST model, which is derived from the Budyko hydrothermal coupling equilibrium hypothesis [42]. The annual WY ($Y(i)$) in pixel i is defined by Equation (6):

$$Y(i) = \left(1 - \frac{AET(i)}{P(i)}\right) \times P(i) \quad (6)$$

where $AET(i)$ (mm yr^{-1}) is the actual evapotranspiration in pixel i and $P(i)$ (mm yr^{-1}) is the annual precipitation in pixel i.

The vegetation evapotranspiration portion of LULC, $\frac{AET(i)}{P(i)}$, is expressed by the Budyko curve, as shown in Equation (7):

$$\frac{AET(i)}{P(i)} = 1 + \frac{PET(i)}{P(i)} - \left[1 + \left(\frac{PET(i)}{P(i)}\right)^{\omega}\right]^{1/\omega} \text{ with : } PET(i) = K_{ij} \times ET_{0,j} \quad (7)$$

where $PET(i)$ is the potential evapotranspiration; $ET_{0,j}$ is the reference evapotranspiration in pixel i; K_{ij} is the vegetation evapotranspiration coefficient of pixel i on LULC; and ω_i is a non-physical parameter that describes the natural climate-soil properties, is defined by Equation (8)

$$\omega_i = Z \times \frac{AWC_i}{P_i} + 1.25 \text{ with : } AWC_i = Min(Re\,st.\,layer, depth, root.depth) \times PAWC \quad (8)$$

where AWC_i (mm) is the volumetric plant-available water content; Z is an empirical constant; and $PAWC$ (mm) is the plant-available water capacity.

For other land use types like water and construction, the actual annual evapotranspiration is calculated by the reference evapotranspiration and has an upper limit defined by the precipitation; the actual annual evapotranspiration (AET_{ij}) is defined by Equation (9):

$$AET_{ij} = Min\left(K_{ij} \times ET_{0,j}, P_i\right) \quad (9)$$

where K_{ij} is the evapotranspiration coefficient of pixel i on LULC; $ET_{0,j}$ (mm yr^{-1}) is the reference evapotranspiration in pixel i; and P_i (mm yr^{-1}) is the annual precipitation in pixel i. The biophysical table was derived from different studies [19]. The parameters of the InVEST model are described in the Supplementary Materials.

2.4.2. Carbon Storage

This module integrates land use/cover classification and distribution within the study area. It uses the carbon density of various carbon pools under different land cover types as foundational data. These densities are multiplied by corresponding land cover areas to calculate carbon stocks of the four major carbon pools within each land cover type. This approach is then used to estimate the total carbon stock across the entire study area. The calculation formula is as follows:

$$C_{total} = C_{above} + C_{below} + C_{soil} + C_{dead} \quad (10)$$

where C_{total}, C_{above}, C_{below}, C_{dead}, and C_{soil} are the total carbon storage, the aboveground biomass carbon density, belowground biomass carbon density, soil organic carbon density, and dead organic matter carbon pools, respectively. The biophysical table was derived from different studies [43,44]. The parameters of the InVEST model are described in the Supplementary Materials.

2.4.3. Waterbirds Habitat Quality

Taking into account the sensitivity of threat factors to different land use practices and the intensity of external threats, factors such as the impact distance and spatial weighting are comprehensively considered in the assessment of habitat conditions under different LULCs. In the output of the habitat quality module, each grid corresponds to a score ranging from 0 to 1, where a higher score indicates higher habitat quality and vice versa. The results were reclassified using natural breaks classification (Jenks) into four categories—excellent (0.9–1), good (0.5–0.9), medium (0.3–0.5), and poor (0–0.3). The main model can be represented as follows:

$$Q_{xj} = H_j \left[1 - \frac{D_{xj}^z}{D_{xj}^z + k^z}\right] \quad (11)$$

$$D_{xj} = \sum_{r=1}^{R} \sum_{y=1}^{yr} \left\{\frac{w_r}{\sum_{r=1}^{R} w_r}\right\} r_y i_{rxy} \beta_x S_{jr} \quad (12)$$

where Q_{xj} is the habitat quality of pixel x for land cover type j and ranges from 0 to 1; H_j is the habitat stress level of pixel x for land cover type j; and k is the half-saturation constant. z is a constant. D_{xj} is the weighted average of the threat level in pixel x. The re-

quired parameters (including threat sources, habitat score, and sensitivity) were obtained from different studies [45]. The parameters of the InVEST model are described in the Supplementary Materials.

2.5. Integrated Ecosystem Services

Due to the inconsistent dimensions of the evaluation results for different ecosystem services, the assessments of three ecosystem services in 2014, 2017, and 2021 were normalized to a range of 0–1. These normalized values were then spatially overlaid using ArcGIS with equal weights. Subsequently, the overall ecosystem service status was reclassified into five categories using the natural breaks (Jenks) classification method: V (1.9–2.2), I (1.4–1.9), III (1.2–1.4), II (0.8–1.2), and I (0–0.8). A higher value indicates better overall ecosystem service status. The integrated ecosystem service (IES) is defined by the following formula:

$$IES = \sum_{j=1}^{3} \frac{ES_{j,k} - ES_{j,min}}{ES_{j,max} - ES_{j,min}} \quad (13)$$

In the equation, $ES_{j,k}$ represents the initial value of ecosystem services j in the grid k; $ES_{j,min}$ and $ES_{j,max}$ denote the minimum and maximum values of ecosystem services, respectively. The number 3 represents the number of investigated ecosystem services.

2.6. Ecosystem Services Trade-Offs and Synergy

2.6.1. Spearman Correlation Analysis

As a widely used rank-based non-parametric test, the Spearman correlation analysis is suitable for both continuous and discrete variables [46]. A Pearson correlation analysis is employed for variables that follow a normal distribution, whereas a Spearman correlation analysis is used for variables that do not follow a normal distribution. Positive and negative coefficients represent cooperative and balancing relationships, respectively. We first created 2000 random points over the study area. The EES values were then extracted for Spearman correlation coefficient (ρ) calculations using the "corrplot" package [47] in R 4.3.3 software.

2.6.2. Spatial Autocorrelation Analysis

Unlike statistical analysis focusing on the variable correlation relationships, spatial autocorrelation analysis examines the degree of spatial dependence between variables. It primarily includes global spatial autocorrelation and local spatial autocorrelation [48]. To reveal the spatial correlations among multiple variables, Anselin [49] introduced bivariate spatial autocorrelation, examining the correlation between one variable and the spatial lag of another variable. The bivariate Moran's I index tests the spatial randomness of the relationship between two variables, and it can be obtained using GeoDa [50]. We divided the study area into 300 m $\times$ 300 m grid data units to explore the spatial aggregation and distribution characteristics of ecosystem services in Dongting Lake. After reassigning the grid values in ArcGIS (version 10.8), the data were imported into GeoDa (GeoDa Version 1.22) software. This study employs Moran's I bivariate local spatial autocorrelation to analyze the spatiotemporal distribution patterns of ecosystem services in Dongting Lake across different PERP stages. It identified trade-offs and synergies at various temporal and spatial scales. The global spatial autocorrelation analysis uses the Moran's I index to assess clustering within the study area, with values ranging $[-1, 1]$. Positive values indicate a positive correlation, while negative values indicate a negative correlation. LISA (local indicator of spatial association) cluster maps, based on Z-values and p-values, represent the association between local multifunctionality and its spatial domain, reflecting existing spatial differences. The results categorize the study area into four clusters: High–High (H–H) and Low–Low (L–L) represent areas of synergy, while High–Low (H–L) and Low–High (L–H) represent areas of trade-off aggregation between paired services. Non-significant areas indicate spatial independence.

The formulas for global (Equation (14)) and local (Equation (15)) Moran's indices are as follows:

$$I = \frac{\sum_{i=1}^{n}\sum_{j=1}^{n} w_{ij}(x_i - \mu)(x_j - \mu)}{\sum_{i=1}^{n}\sum_{j=1}^{n} w_{ij}\sum_{i=1}^{n}(x_i - \mu)^2} \quad (14)$$

$$I_i = \frac{x_i - \mu}{S^2}\sum_{j=1}^{n} w_{ij}(x_{ij} - \mu) \quad (15)$$

where i is the spatial relationship between the bivariate variables, w_{ij} is the spatial weight matrix, n is the number of spatial units, $x_{i(j)} - \mu$ is the deviation of the observed value from the mean of the spatial units $i(j)$, and S^2 is the variance. LISA cluster maps were analyzed using GeoDa 1.22 software and further processed and mapped using ArcGIS 10.8 software.

3. Results

3.1. Land Use and Land Cover Change

The distribution of Dongting Lake wetland types during the PERP was shown in Figure 2. The RF classifier had very high performance with an overall accuracy of ≥90% and Kappa coefficient of ≥0.9 for all years. These high-accuracy wetland maps ensured the reliability of subsequential ESS evaluation.

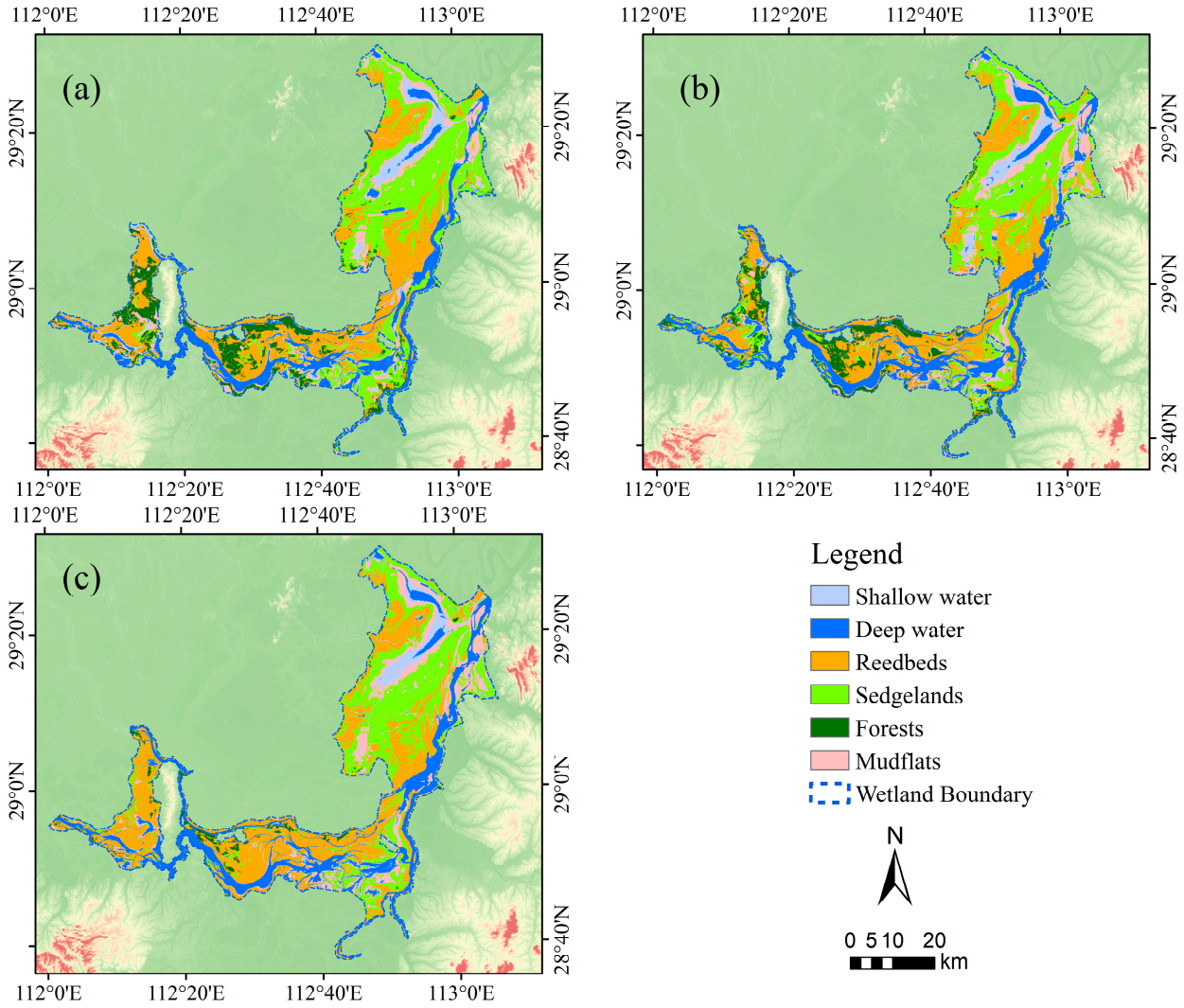


Figure 2. Wetland types in Dongting Lake before (**a**), during (**b**), and after (**c**) the Poplar Ecological Restoration Project.

Over the period of PERP, a total of 20,357 ha (82.95%) of poplar forests were removed and transferred to other wetland types, and these changes mainly occurred during 2014–2021 (Table 3). The pixel-by-pixel comparison revealed that the majority of forests were replaced by reedbeds (17,404 ha), followed by sedgelands (3841 ha), mudflats (443 ha), shallow waters (382 ha), and deep waters (301 ha). Moreover, there were also exchanges among other wetland types during the period, such as reedbeds being replaced by sedgelands and vice versa. The changes in wetland types were quantified as total gains, total losses, and persistence [51], which is presented in the Supplementary Materials.

Table 3. Wetland area (ha) transitions in Dongting Lake during 2014–2021.

	Area (%) in 2014	Area (%) in 2017	Area (%) in 2021	Overall Gain (Loss)
Forests	24,540 (9.27)	18,414 (7.35)	4183 (1.67)	−20,357 (−82.95)
Reedbeds	69,100 (27.58)	70,133 (27.99)	85,659 (34.19)	16,559 (23.96)
Sedgelands	74,164 (29.60)	65,053 (25.96)	68,325 (27.27)	−5839 (−7.87)
Mudflats	24,798 (9.90)	30,533 (12.19)	32,143 (12.83)	7345 (29.62)
Shallow waters	22,168 (8.85)	17,717 (7.07)	16,343 (6.52)	−5825 (−26.28)
Deep waters	35,782 (14.28)	48,702 (19.44)	43,897 (17.52)	8115 (22.68)

3.2. Spatiotemporal Variations of Ecological Services

The spatiotemporal patterns of ecosystem services in Dongting Lake are presented and described, with the changes in wetland types being shown in Supplementary Materials Figure S1.

3.2.1. Changes in Water Conservation

With the changes in wetland type, Dongting Lake exhibited different characteristics in terms of overall water conservation (Table 4). The total water conservation amounts were 1.61 km^3, 1.53 km^3, and 1.60 km^3 for 2014, 2017, and 2021, respectively. The overall trend of total water conservation from 2014 to 2021 showed a decrease followed by an increase, with a total reduction of 0.01 km^3 and a decrease rate of 0.63%. Nevertheless, the water conservation amount in PERP areas gradually increased with the removal of poplar forests (Table 4). The inconsistency was caused by the distinct water conservation capacity of different wetland types specified in the InVEST model. RB, ML, and DW had clear increases in total water conservation amounts, while FR, SW, and SL showed decreasing trends. The changes in total water conservation amounts for different wetland types were consistent with their respective area change trends.

Table 4. The characteristics of water conservation changes in Dongting Lake.

Year	Water Conservation of Each Wetland Types (km^3)						Total	Water Conservation in Deforested Area
	SW	DW	RB	SL	FR	ML	(km^3)	
2014	0.02	0.03	0.66	0.61	0.17	0.12	1.61	0.16
2017	0.01	0.04	0.67	0.53	0.13	0.15	1.53	0.17
2021	0.01	0.03	0.81	0.56	0.03	0.16	1.60	0.19
Change (km^3)	−0.01	0	0.15	−0.05	−0.14	0.04	−0.01	0.03
Change (%)	−50	0	22.73	−8.20	−82.35	33.3	−0.62	18.75

3.2.2. Changes in Cabon Storage

With the removal of Poplar forests, the average carbon storage capacity decreased in Dongting Lake. The unit carbon storage was 108.58 MG/ha, 96.32 MG/ha, and 84.65 MG/ha in 2014, 2017, and 2021, respectively (Figure S1d, S1e, and S1f). From a spatial distribution perspective, high-value areas of lake carbon storage were mainly concentrated in the southwest region of the Lake, which had more forests and reedbeds. Under the influence of PERP, as forest area decreased, total lake carbon storage decreased from 2.72×10^7 MG in 2014 to 2.41×10^7 MG in 2017 (an average decrease rate of 1.03×10^6 MG·yr^{-1}). The carbon

storage capacity continued to decline to 2.12×10^7 MG in 2021 (an average decrease rate of 7.25×10^5 MG·yr^{-1}). This reduction mainly occurred in the core area of the Dongting Lake Protection Area. Further observations of carbon storage for each wetland type revealed that FR had the highest value (393 MG/ha), followed by RB (154.58 MG/ha).

3.2.3. Changes in Habitat Quality

The average habitat quality score was 0.701, 0.688, and 0.705 for 2014, 2017, and 2021, respectively (Figure S1g, S1h, and S1i). Based on the habitat degradation index provided by the habitat quality module, the maximum values were 0.453, 0.499, and 0.469 in 2014, 2017, and 2021, respectively, and the corresponding mean values were 5.296×10^{-2}, 5.338×10^{-2}, and 5.339×10^{-2}. This indicates an overall increase in the risk of habitat degradation over time and highlights that local degradation risks should not be ignored. The proportion of areas assessed as medium-grade changed notably from 43.26% in 2014 to 48.69% in 2017 and further increased to 51.67% in 2021 (Table 5). Areas classified as poor experienced a considerable decrease from 8.14% in 2014 to 5.96% in 2017 and reached 1.58% by 2021 (Table 5). The proportion of areas classified as good remained relatively stable (Table 5). Excellent-grade areas decreased from 35.05% in 2014 to 30.58% in 2017 but maintained stability at around 31.43% in 2021 (Table 5). Overall, the PERP led to a transformation of most poor-grade areas into medium-grade ones (Figure S1g, S1h, and S1i) and improved the overall habitat quality levels in the lake.

Table 5. Temporal changes in different habitat quality levels of Dongting Lake from 2014 to 2021.

	2014		2017		2021	
	Area (ha)	**%**	**Area (ha)**	**%**	**Area (ha)**	**%**
Poor	20,390.31	8.14	14,926.05	5.96	3957.48	1.58
Medium	108,391.05	43.26	122,009.49	48.69	129,457.89	51.67
Good	33,972.03	13.56	37,003.14	14.77	38,408.04	15.33
Excellent	87,814.08	35.05	76,628.79	30.58	78,744.06	31.43

3.2.4. Changes in Integrated Ecosystem Service

The average IES index in Dongting Lake was 1.560, 1.479, and 1.494 in 2014, 2017, and 2021, respectively, showing a slight downward trend in IESs (Figure S2, Table 6). The high-IES areas were mainly distributed in SL and FR, reflecting their higher carbon storage capacity and high habitat quality.

Table 6. Temporal changes in different IES levels of Dongting Lake from 2014 to 2021.

	2014		2017		2021	
	Area (ha)	**%**	**Area (ha)**	**%**	**Area (ha)**	**%**
I	35,855	14.31	48,806	19.48	43,967	17.55
II	24,256	9.68	19,847	7.92	17,906	7.15
III	22,998	9.18	28,446	11.35	30,664	12.24
IV	101,198	40.39	104,088	41.54	113,151	45.16
V	66,261	26.44	49,380	19.71	44,879	17.91

3.3. Ecosystem Services Trade-Offs and Synergies

3.3.1. Ecological Services Are Highly Correlated

The Spearman correlation analysis showed that there were significant differences in the trade-offs and synergies among different ecosystem services in the Dongting Lake ecosystem, and the intensity of these trade-offs and synergies changes over time (Table 7). Specifically, there has been a consistently strong positive correlation between WC and CS, indicating a strong synergy between them. Furthermore, this synergy has gradually increased with the implementation of PERP. On the other hand, there has been a consistently

strong negative correlation between CS and HQ, suggesting a significant trade-off relationship between them that has gradually weakened with PERP implementation. For WC and HQ, there was a significant negative correlation in 2014; however, with the implementation of PERP, the strength of this relationship weakened (−0.02 in 2017 and −0.04 in 2021, $p > 0.05$, Table 7).

Table 7. Correlation coefficients between WC, CS, and HQ.

Year	WC vs. CS	WC vs. HQ	CS vs. HQ
2014	0.76 **	−0.05 *	−0.41 **
2017	0.82 **	−0.02	−0.28 **
2021	0.86 **	−0.04	−0.22 **

Note: * represents the significant correlation of data at the 0.05 level; ** represents that the data are significantly correlated at the 0.01 level; unmarked represents that the significant *p*-value is greater than 0.05.

3.3.2. Clusters and Spatial Heterogeneity of Ecological Services

Global Autocorrelation Analysis

The global autocorrelation analysis showed that the EESs had a significant Moran's I with a *p*-value of 0.001 for all paired comparations in every year except between WC and HQ in 2014. The significance was confirmed with the permutation tests (Table 8). The overall spatial relationship between WC and CS exhibited a significantly positive correlation, with the correlation strengthening over time. CS and HQ exhibit a significant negative correlation in spatial terms, with the correlation gradually weakening over time.

Table 8. Results of bivariate spatial correlation analysis for ecosystem services in Dongting Lake.

	2014		2017		2021	
	Moran's I	Z-Score	Moran's I	Z-Score	Moran's I	Z-Score
WC vs. CS	0.474 **	185.68	0.533 **	205.51	0.627 **	232.07
WC vs. HQ	−0.004	−1.91	0.030 **	13.93	0.011 **	4.89
CS vs. HQ	−0.437 **	−183.27	−0.359 **	−155.52	−0.274 **	−124.32

Note: ** indicates significant correlation at the 0.01 level; an unmarked Moran's I represents the absence of spatial autocorrelation.

Local Autocorrelation Analysis

The results of the local bivariate spatial autocorrelation analysis indicated that there was high spatial heterogeneity (i.e., clusters of trade-offs and synergies between EES) in Dongting Lake (Table 9, Figure 3). Moreover, this clustering was strengthened under PERP as the areas with spatial randomness decreased over time for all paired analyses (Table 9).

Table 9. Changes in the trade-off and synergy relationships of ecosystem services from 2014 to 2021 in Dongting Lake. The dominant association is in bold.

	WC and CS (%)			WC and HQ (%)			CS and HQ (%)		
	2014	2017	2021	2014	2017	2021	2014	2017	2021
Not significant	58.18	53.35	45.85	32.30	32.87	30.88	32.30	32.87	30.88
High–High	10.11	13.94	24.10	22.61	20.03	20.03	1.04	2.76	15.74
Low–Low	25.07	28.16	26.50	12.58	15.42	14.98	8.98	13.06	13.68
Low–High	4.29	2.80	1.66	9.76	10.82	11.48	31.33	28.09	15.77
High–Low	2.35	1.75	1.89	22.76	20.86	22.64	26.35	23.22	23.93
Synergy	35.18	42.10	50.60	35.19	35.45	35.01	10.02	15.82	29.42
Trade-off	6.64	4.55	3.54	32.51	31.67	34.12	57.68	51.31	39.70

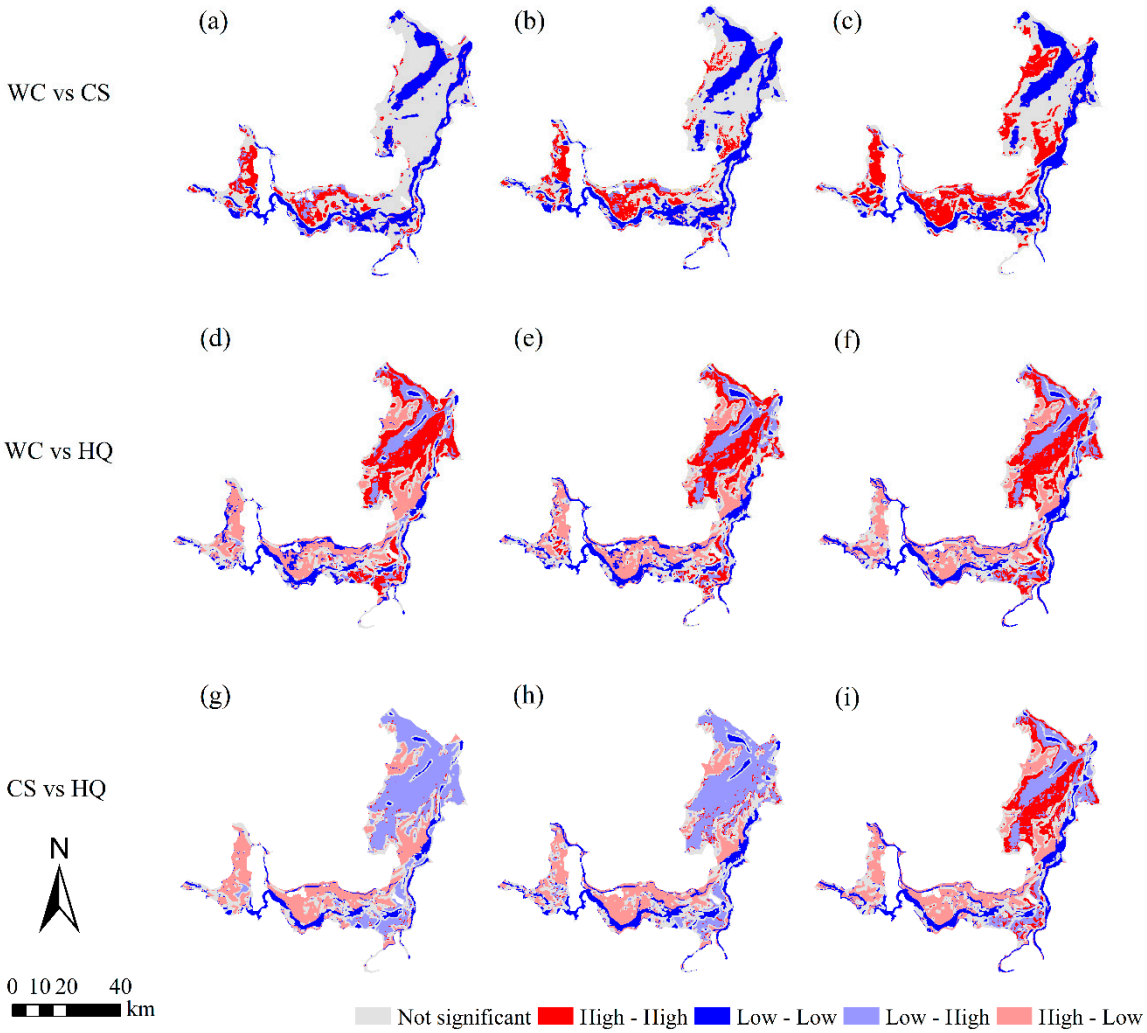


Figure 3. LISA cluster maps showing the spatial correlation between ecological services. (**a**) WC vs. CS in 2014, (**b**) WC vs. CS in 2017, (**c**) WC vs. CS in 2021, (**d**) WC vs. HQ in 2014, (**e**) WC vs. HQ in 2017, (**f**) WC vs. HQ in 2021, (**g**) CS vs. HQ in 2014, (**h**) CS vs. HQ in 2017, and (**i**) CS vs. HQ in 2021.

Between WC and CS, spatial randomness dominated the landscape. Nonetheless, considerable areas had synergetic relationships (>35%) and a small amount of areas had trade-off relationships (<10%) (Table 9). Moreover, of the areas with positive associations, Low–Low relationship dominated, although the areas with High–High association increased considerably. Between WC and HQ, the areas with random, positive, and negative associations were quite similar for before, during, and after PERP (Table 9), suggesting that PERP had little efforts on the spatial association between WC and HQ. For CS and HQ, there were more areas with synergetic relationships, and positive relationships became dominant post-PERP (53.86%, Table 9).

4. Discussion

Assessing ecological restoration projects is critical for determining their effectiveness and guiding future efforts. Using Dongting Lake as a case study, this study systematically evaluated the ESS outcomes by quantifying three key ESSs, including water conservation, carbon storage, and habitat quality before, during, and after the implementation of the PERP. Moreover, we explored and mapped the clusters of trade-offs and synergies between ESSs through bivariate spatial autocorrelation analyses. We found that while the water conservation and carbon storage decreased, habitat quality was improved and IESs decreased slightly. Moreover, PERP increased ESS synergies and reduced the ESS trade-offs.

4.1. Land Use and Land Cover Changes

The spatiotemporal distribution patterns of LULC varied dramatically in Dongting Lake before and after the PERP. The most notable change was the reduction in plantation, which was mainly replaced by reedbeds and sedgelands. As the plantations mainly occurred at higher elevation, the deforestation provided spaces and the hydrological condition for the rapid colonization of highly invasive plants, such as common reed [52,53] and canary grass [54]. A previous study also found that the deforested areas primarily transitioned to reedbeds and sedgelands [55,56].

We also found that there were notable interchanges among wetland types during PERP, especially between RB and SL. These changes, mainly found in areas close to river banks and lake shore, might be facilitated by the removal of poplar plantation due to the increased erosion [57]. Although exploring the impacts of PERP on vegetation change is out of the scope of this study, it should be part of the evaluation of the ecological restoration project.

4.2. Temporal and Spatial Variations of Ecosystem Services

During the various stages of the PERP, the overall water conservation capacity initially declined before increasing, reflecting changes in surface water levels in Dongting Lake from 2014 to 2017 [53]. Although the lake's total water conservation capacity decreased slightly (0.62%), it increased significantly (18.75%) in the PERP-affected areas. This rise is likely due to the higher evapotranspiration rates associated with poplar forests compared with herbaceous wetland vegetation, as well as the lower soil moisture content in these regions [58,59]. These changes can be attributed to a reduction in land area and an increase in water surface area within the Dongting Lake region. As land area decreases, the vegetation available to intercept rainfall also declines, reducing overall water conservation capacity. This trend is common in global wetland restoration projects. For example, the Baiyangdian Wetland saw significant improvement in water supply capacity following the implementation of ecological restoration measures. Both ecological water replenishment (EWR) and the PERP share a similar goal of enhancing water resource availability: EWR increases overall water yield by replenishing water resources, while the PERP promotes a shift toward more water-efficient vegetation by removing less efficient poplar trees [60]. Both initiatives aim to improve the ecosystem's hydrological conditions and promote sustainable water resource management. However, it is important to consider that higher temperatures, deeper root systems, and actual evapotranspiration rates may negatively affect water resource services. Comparisons between the effects of the PERP in Dongting Lake and other wetland restoration projects, such as the study by Hu et al. [61], indicate that changes in landscape patterns significantly enhance wetland water supply services, providing valuable insights into the ecological benefits of such projects.

The succession and growth of trees directly threaten many shade-intolerant herbaceous species, complicating their survival due to increased competition for resources [62]. The study found that areas of "Good" or higher habitat quality were primarily associated with shallow waters and sedgelands, which serve as key foraging habitats for overwintering migratory waterbirds, including geese, ducks, plovers, and sandpipers [63]. Plovers and sandpipers predominantly inhabit mudflats and shallow waters, while most geese and ducks rely heavily on sedgelands and shallow waters, with only a few diving ducks foraging in deeper waters. In terms of habitat quality, areas of poor quality were predominantly reedbeds, with forests showing the lowest habitat quality, aligning with the findings of Liu et al. [64]. The principles of the PERP in enhancing habitat quality are similar to those of other wetland restoration projects aimed at benefiting waterfowl. For instance, studies by Kang et al. [65] show that wetland restoration can improve bird habitats. Likewise, sediment retention and restoration projects around the Yangtze River estuary [66] seek to expand habitat and food resources for waterfowl. While the PERP has improved habitat quality, for example, Qu et al. [67] found that it significantly enhanced habitat suitability for migratory birds from the Anatidae and Ardeidae families. However, between 2014 and 2017, there was a significant increase in roads and impervious surfaces within 1 km of Dongting Lake, while

farmland areas remained relatively unchanged. Roads and impervious surfaces are known to negatively impact habitat quality [56]. Although the PERP improved habitat conditions, overall habitat quality from 2014 to 2017 continued to decline due to the negative effects of degradation threats outweighing the positive impacts of the PERP.

The study revealed a slight decline in Integrated Ecosystem Services (IESs) in Dongting Lake following the implementation of the PERP, indicating that the PERP alone cannot fully counteract the negative effects of accelerating climate change and ongoing human disturbances. Moreover, wetlands provide a wide range of valuable ecosystem services, but this study focused on only three key services. Other important services, such as water quality improvement and cultural services, were not evaluated, which limits the study's ability to capture the full spectrum of benefits provided by Dongting Lake or the effectiveness of the PERP. Further research encompassing a broader range of ecosystem services is needed to fully assess the overall ecological impact of the PERP and similar restoration efforts.

4.3. Trade-Offs and Synergies of Ecosystem Services

There was a significant positive correlation between WC and CS services over time. Spatially, WC and CS exhibited a strong synergistic relationship. In wetlands, WC mainly accumulates in higher-elevation areas with dense vegetation cover, and regions with high carbon storage are primarily located where vegetation growth is prominent. These findings align with those of Yue et al. [68]. As PERP progressed, synergistic areas—primarily found in sedgelands—within Dongting Lake increased. The rapid colonization of deforested area by sedgeland plants likely contributed to simultaneous improvements in WC and CS, as vegetation such as sedges can effectively sequester carbon and intercept significant rainfall [69].

There was no significant correlation between WC and HQ over time; however, spatially, the relationship shifted from non-significant to significantly positive. This shift may be attributed to the role of increased WC in regulating water levels in Dongting Lake, as the total number of migratory waterbirds is significantly correlated with water levels [70]. Changes in wetland water levels directly influence the distribution of suitable bird habitats [71]. Early or delayed water level withdrawal affects the extent of exposed lakebed, having negative impacts on the development of annual wet meadows (such as Carex), reducing the availability of suitable feeding areas and thereby diminishing foraging habitats for overwintering birds [72]. For instance, the early retreat of water levels in Dongting Lake prompted the lesser white-fronted goose to concentrate in sub-lakes with managed water levels [73]. The implementation of PERP likely enhanced wetland ecological functions, thereby strengthening the correlation between water conservation and habitat quality.

There was a significant negative correlation between carbon storage (CS) and habitat quality (HQ) services over time. Spatially, CS and HQ exhibited a strong trade-off relationship. While deforestation initially reduced carbon storage, as forests generally store more carbon than other land covers [74], it created the conditions for a long-term improvement in habitat quality. As habitat quality began to recover and improve through the colonization of wetland plants, carbon storage gradually increased [75], leading to an expansion of areas showing High–High synergy.

However, this study highlights a critical gap in the quantitative analysis of the mechanisms driving trade-offs and synergies among ecosystem services. More detailed and long-term assessments of these services are needed to fully understand the impacts of ecological restoration projects. This research addresses the trade-off between tree planting and wetland conservation in the Dongting Lake wetland ecosystem, consistent with findings from a 2000–2016 study on the impact of afforestation on wetland dynamics in China, which emphasized the varied hydrological consequences of tree planting on wetland ecosystems [76]. By elucidating the complex interplay between afforestation and wetland conservation, this study provides valuable insights for shaping future ecological restoration strategies.

4.4. Limitations and Future Outlooks

There are three key limitations that warrant attention in future research to broaden the scope of studies in this field. First, the research relies on subjective judgment and survey results to independently evaluate three ecosystem services. Current studies on wetland ecosystem services often lack standardized indicators, which hampers the comparability of specific services across different regions [58]. This issue stems from data gaps and the complexities involved in the creation, exchange, and quantification of cultural services. The absence of standardized assessment criteria for wetland ecosystem services exacerbates this complexity [15]. Furthermore, the Integrated Ecosystem Services (IESs) measure used in this study is derived solely from a simple aggregation of the three evaluated ecosystem services and does not encompass cultural services, which limits its applicability. Future studies should broaden the range of services considered and enhance the IES assessment framework to improve the reliability of research on cross-regional ecosystem service mechanisms. Second, this study aims to reveal the impact of land use changes driven by the PERP on ecosystems. Although meteorological data were fixed during simulations to isolate the effects of LULC changes, other driving factors, such as climate and socio-economic variables, also influence land use patterns. Additionally, various factors may affect the formation and variation of recent land use patterns, highlighting the need for further investigation into the impacts of these additional factors on environmental services. Third, despite the widespread use of the InVEST model for ecosystem service assessment, certain limitations persist in its evaluations. For instance, in the habitat quality module, the weights assigned to threat factors, maximum impact distances, and habitat suitability scores are largely based on empirical values and expert judgment, introducing subjectivity [77]. While previous studies have optimized some parameters, there remains significant room for improvement. To address this limitation, future research should consider comparing or integrating the InVEST model with other ecological process models or calibrating habitat assessments using field surveys.

5. Conclusions

Using the InVEST model, including the water yield, carbon storage, and habitat quality modules, combined with geostatistical methods, we effectively evaluated the status of water conservation, carbon storage, and habitat quality services in the Dongting Lake wetlands before, during, and after the PERP. From 2014 to 2021, as the PERP was implemented, large areas of poplar plantations transitioned to RBs and SLs. With these land cover changes, water conservation and habitat quality initially decreased but then increased, while carbon storage consistently declined. In the PERP implementation areas, all services except carbon storage showed local improvement. Despite the PERP contributing to the maintenance of the lake's environment (such as more natural water levels) and biodiversity (including habitat improvements), the cost of carbon storage outweighed the benefits of water conservation and habitat quality, resulting in a slight decrease in the integrated ecosystem services. These findings highlight the importance of setting clear restoration priorities and targets, as well as balancing the diverse ecosystem services. Furthermore, our results showed that the temporal and spatial patterns of trade-offs and synergies of the ecosystem services changed significantly, with synergistic areas continuously expanding. More importantly, the synergetic association shifted to positive post-PERP. These findings indicate that multiple services can be enhanced simultaneously, leading to overall ecosystem resilience and sustainability.

Supplementary Materials: The following supporting information can be downloaded at: https://www.mdpi.com/article/10.3390/rs16214062/s1, Table S1: Data requirements for the water yield module. Table S2: Data requirements for the carbon storage and sequestration module. Table S3: Data requirements for the habitat quality module: threat factor-related data. Table S4: Data requirements for the habitat quality module: habitat types and their sensitivity to threats. Table S5: The gain, loss, and persistence for Dongting Lake wetland types from 2014 to 2021. Figure S1: Spatial patterns of ecosystem services in Dongting Lake for water conservation (a, b, and c), carbon storage

(d, e, and f), and habitat quality (g, h, and i) before, during, and after the poplar ecological restoration project. Figure S2. Spatiotemporal pattern of integrated ecosystem services in Dongting Lake for 2014 (a), 2017 (b), and 2021 (c).

Author Contributions: Conceptualization, J.Z., L.W., C.L. and J.X.; methodology, J.Z. and L.W.; software, J.Z. and J.X.; validation, J.Z., G.L. and L.W.; formal analysis, Z.W. and C.L.; investigation, J.Z., Y.H., Z.W. and P.L.; data curation, J.Z., Y.H. and Z.W.; writing—original draft preparation, J.Z.; writing—review and editing, G.L. and L.W.; visualization, J.X. and C.L.; supervision, L.W.; project administration, L.W. and G.L.; funding acquisition, L.W. and G.L. All authors have read and agreed to the published version of the manuscript.

Funding: This research was funded by the Joint Fund for Regional Innovation and Development of NSFC (U22A20563), Major Water Conservancy Science and Technology Projects in Hunan Province (XSKJ2023059-05), and Science and Technology Platform Project of Hunan Province (2022PT1010).

Data Availability Statement: The data are contained within the article or Supplementary Materials.

Acknowledgments: We are grateful for comments from four anonymous reviewer.

Conflicts of Interest: The authors declare no conflicts of interest.

References

1. Turner, R.K.; Van Den Bergh, J.C.; Söderqvist, T.; Barendregt, A.; Van Der Straaten, J.; Maltby, E.; Van Ierland, E.C. Ecological-economic analysis of wetlands: Scientific integration for management and policy. *Ecol. Econ.* **2000**, *35*, 7–23. [CrossRef]
2. Villa, J.A.; Bernal, B. Carbon sequestration in wetlands, from science to practice: An overview of the biogeochemical process, measurement methods, and policy framework. *Ecol. Eng.* **2018**, *114*, 115–128. [CrossRef]
3. Xiong, Y.; Mo, S.; Wu, H.; Qu, X.; Liu, Y.; Zhou, L. Influence of human activities and climate change on wetland landscape pattern—A review. *Sci. Total Environ.* **2023**, *879*, 163112. [CrossRef] [PubMed]
4. Hu, S.; Niu, Z.; Chen, Y. Global wetland datasets: A review. *Wetlands* **2017**, *37*, 807–817. [CrossRef]
5. Riley, W.D.; Potter, E.C.; Biggs, J.; Collins, A.L.; Jarvie, H.P.; Jones, J.I.; Kelly-Quinn, M.; Ormerod, S.J.; Sear, D.A.; Wilby, R.L. Small Water Bodies in Great Britain and Ireland: Ecosystem function, human-generated degradation, and options for restorative action. *Sci. Total Environ.* **2018**, *645*, 1598–1616. [CrossRef]
6. Paulson Institute. *Blueprint of Coastal Wetland Conservation and Management in China*; Institute of Geographic Sciences Natural Resources Research, CAS: Beijing, China; Higher Education Press: Beijing, China, 2016.
7. Dungan, P.J. *Wetland Conservation: A Review of Current Issues and Required Action*; IUCN: Gland, Switzerland, 1990; pp. 23–34.
8. Kingsford, R.T.; Basset, A.; Jackson, L. Wetlands: Conservation's poor cousins. *Aquat. Conserv. Mar. Freshw. Ecosyst.* **2016**, *26*, 892–916. [CrossRef]
9. Murcia, C.; Guariguata, M.R.; Andrade, Á.; Andrade, G.I.; Aronson, J.; Escobar, E.M.; Etter, A.; Moreno, F.H.; Ramírez, W.; Montes, E. Challenges and Prospects for Scaling-up Ecological Restoration to Meet International Commitments: Colombia as a Case Study. *Conserv. Lett.* **2016**, *9*, 213–220. [CrossRef]
10. Kareiva, P. *Natural Capital: Theory and Practice of Mapping Ecosystem Services*; Oxford University Press: New York, NY, USA, 2011; pp. 13–36.
11. Natural Capital ProjectInVEST 3.14.2. Stanford University, University of Minnesota, Chinese Academy of Sciences, The Nature Conservancy, World Wildlife Fund, Stockholm Resilience Centre and the Royal Swedish Academy of Sciences. Available online: https://naturalcapitalproject.stanford.edu/software/invest (accessed on 24 January 2024).
12. Terrado, M.; Sabater, S.; Chaplin-Kramer, B.; Mandle, L.; Ziv, G.; Acuña, V. Model development for the assessment of terrestrial and aquatic habitat quality in conservation planning. *Sci. Total Environ.* **2016**, *540*, 63–70. [CrossRef]
13. Xu, X.; Chen, M.; Yang, G.; Jiang, B.; Zhang, J. Wetland ecosystem services research: A critical review. *Glob. Ecol. Conserv.* **2020**, *22*, e01027. [CrossRef]
14. Yang, Y.; Xiao, P.; Feng, X.; Li, H. Accuracy assessment of seven global land cover datasets over China. *ISPRS J. Photogramm. Remote Sens.* **2017**, *125*, 156–173. [CrossRef]
15. Xu, X.; Jiang, B.; Tan, Y.; Costanza, R.; Yang, G. Lake-wetland ecosystem services modeling and valuation: Progress, gaps and future directions. *Ecosyst. Serv.* **2018**, *33*, 19–28. [CrossRef]
16. Li, Y.; Chen, X.; Xie, Y.; Li, X.; Li, F.; Hou, Z. Effects of young poplar plantations on understory plant diversity in the Dongting Lake wetlands, China. *Sci. Rep.* **2014**, *4*, 6339. [CrossRef] [PubMed]
17. Lei, J.; Cai, L.; Yan, Z.; Ao-jie, Z.; Guang-chun, L. Spatio-temporal characteristics of the expansion of poplar plantation in West Dongting Lake wetland, China. *Chin. J. Appl. Ecol.* **2016**, *27*, 2039–2047. [CrossRef]
18. Li, Y.; Qin, H.; Xie, Y.; Wang, W.; Chen, X.; Zhang, C. Physiological mechanism for the reduction in soil water in poplar (*Populus deltoides*) plantations in Dongting Lake wetlands. *Wetl. Ecol. Manag.* **2014**, *22*, 25–33. [CrossRef]
19. Hu, W.; Li, G.; Gao, Z.; Jia, G.; Wang, Z.; Li, Y. Assessment of the impact of the Poplar Ecological Retreat Project on water conservation in the Dongting Lake wetland region using the InVEST model. *Sci. Total Environ.* **2020**, *733*, 139423. [CrossRef]

20. Wu, H.; Xiao, S.; Dai, J.; Xiong, Y.; Cao, J.; Qu, X.; Wang, G.; Yang, R. Effect of poplar ecological retreat project on soil bacterial community structure in Dongting Lake wetland. *Front. Microbiol.* **2022**, *13*, 1026872. [CrossRef]
21. Goldstein, J.H.; Caldarone, G.; Duarte, T.K.; Ennaanay, D.; Hannahs, N.; Mendoza, G.; Polasky, S.; Wolny, S.; Daily, G.C. Integrating ecosystem-service tradeoffs into land-use decisions. *Proc. Natl. Acad. Sci. USA* **2012**, *109*, 7565–7570. [CrossRef]
22. Adam, E.; Mutanga, O.; Rugege, D. Multispectral and hyperspectral remote sensing for identification and mapping of wetland vegetation: A review. *Wetl. Ecol. Manag.* **2010**, *18*, 281–296. [CrossRef]
23. Gao, X.; Liang, J.; Zhu, Z.; Li, W.; Lu, L.; Li, X.; Li, S.; Tang, N.; Li, X. Drought-induced changes in hydrological and phenological interactions modulate waterbird habitats dynamics. *J. Hydrol.* **2023**, *626*, 130228. [CrossRef]
24. Jing, L.; Zeng, Q.; He, K.; Liu, P.; Fan, R.; Lu, W.; Lei, G.; Lu, C.; Wen, L. Vegetation dynamic in a large floodplain wetland: The effects of hydroclimatic regime. *Remote Sens.* **2023**, *15*, 2614. [CrossRef]
25. Liu, Y.; Li, J.; Yan, D.; Chen, L.; Li, M.; Luan, Z. Typical vegetation dynamics and hydrological changes of Dongting Lake wetland from 1985 to 2020. *Ecohydrol. Hydrobiol.* **2023**. [CrossRef]
26. Long, X.; Li, X.; Lin, H.; Zhang, M. Mapping the vegetation distribution and dynamics of a wetland using adaptive-stacking and Google Earth Engine based on multi-source remote sensing data. *Int. J. Appl. Earth Obs. Geoinf.* **2021**, *102*, 102453. [CrossRef]
27. Tran, T.V.; Reef, R.; Zhu, X. A Review of Spectral Indices for Mangrove Remote Sensing. *Remote Sens.* **2022**, *14*, 4868. [CrossRef]
28. Tucker, C.J. Red and photographic infrared linear combinations for monitoring vegetation. *Remote Sens. Environ.* **1979**, *8*, 127–150. [CrossRef]
29. Xu, H. Modification of normalised difference water index (NDWI) to enhance open water features in remotely sensed imagery. *Int. J. Remote Sens.* **2006**, *27*, 3025–3033. [CrossRef]
30. Gitelson, A.A.; Kaufman, Y.J.; Merzlyak, M.N. Use of a green channel in remote sensing of global vegetation from EOS-MODIS. *Remote Sens. Environ.* **1996**, *58*, 289–298. [CrossRef]
31. Diek, S.; Fornallaz, F.; Schaepman, M.E.; De Jong, R. Barest pixel composite for agricultural areas using landsat time series. *Remote Sens.* **2017**, *9*, 1245. [CrossRef]
32. Mourad, R.; Jaafar, H.; Anderson, M.; Gao, F. Assessment of leaf area index models using harmonized landsat and sentinel-2 surface reflectance data over a semi-arid irrigated landscape. *Remote Sens.* **2020**, *12*, 3121. [CrossRef]
33. Henderson, F.M.; Lewis, A.J. Radar detection of wetland ecosystems: A review. *Int. J. Remote Sens.* **2008**, *29*, 5809–5835. [CrossRef]
34. Mahdavi, S.; Salehi, B.; Granger, J.; Amani, M.; Brisco, B.; Huang, W. Remote sensing for wetland classification: A comprehensive review. *GIScience Remote Sens.* **2018**, *55*, 623–658. [CrossRef]
35. Araya, S.; Ostendorf, B.; Lyle, G.; Lewis, M. CropPhenology: An R package for extracting crop phenology from time series remotely sensed vegetation index imagery. *Ecol. Inform.* **2018**, *46*, 45–56. [CrossRef]
36. Sakamoto, T.; Yokozawa, M.; Toritani, H.; Shibayama, M.; Ishitsuka, N.; Ohno, H. A crop phenology detection method using time-series MODIS data. *Remote Sens. Environ.* **2005**, *96*, 366–374. [CrossRef]
37. R Development Core Team. *R: A Language and Environment for Statistical Computing*; R Foundation for Statistical Computing: Vienna, Austria, 2022.
38. Talukdar, S.; Singha, P.; Mahato, S.; Pal, S.; Liou, Y.-A.; Rahman, A. Land-use land-cover classification by machine learning classifiers for satellite observations—A review. *Remote Sens.* **2020**, *12*, 1135. [CrossRef]
39. Berhane, T.M.; Lane, C.R.; Wu, Q.; Autrey, B.C.; Anenkhonov, O.A.; Chepinoga, V.V.; Liu, H. Decision-tree, rule-based, and random forest classification of high-resolution multispectral imagery for wetland mapping and inventory. *Remote Sens.* **2018**, *10*, 580. [CrossRef] [PubMed]
40. Ghosh, S.; Das, A. Wetland conversion risk assessment of East Kolkata Wetland: A Ramsar site using random forest and support vector machine model. *J. Clean. Prod.* **2020**, *275*, 123475. [CrossRef]
41. Teng, J.; Xia, S.; Liu, Y.; Yu, X.; Duan, H.; Xiao, H.; Zhao, C. Assessing habitat suitability for wintering geese by using Normalized Difference Water Index (NDWI) in a large floodplain wetland, China. *Ecol. Indic.* **2021**, *122*, 107260. [CrossRef]
42. Donohue, R.J.; Roderick, M.L.; McVicar, T.R. Roots, storms and soil pores: Incorporating key ecohydrological processes into Budyko's hydrological model. *J. Hydrol.* **2012**, *436–437*, 35–50. [CrossRef]
43. An, X.; Jin, W.; Long, X.; Chen, S.; Qi, S.; Zhang, M. Spatial and temporal evolution of carbon stocks in Dongting Lake wetlands based on remote sensing data. *Geocarto Int.* **2022**, *37*, 14983–15009. [CrossRef]
44. Long, W.; Zhi, L.; Guo, Y. Analysis of spatiotemporal evolution and contribution factors of carbon storage in the West Dongting Lake Nature Reserve in the past 20 years. *Remote Sens. Nat. Resour.* **2024**, 1–11. [CrossRef]
45. Sun, C.; König, H.J.; Uthes, S.; Chen, C.; Li, P.; Hemminger, K. Protection effect of overwintering water bird habitat and defining the conservation priority area in Poyang Lake wetland, China. *Environ. Res. Lett.* **2020**, *15*, 125013. [CrossRef]
46. Hauke, J.; Kossowski, T. Comparison of values of Pearson's and Spearman's correlation coefficients on the same sets of data. *Quaest. Geogr.* **2011**, *30*, 87–93. [CrossRef]
47. Wei, T.; Simko, V.; Levy, M.; Xie, Y.; Jin, Y.; Zemla, J. Package 'corrplot'. *Statistician* **2017**, *56*, e24.
48. Cliff, A.D.; Ord, J.K. *Spatial Autocorrelation*; Pion: London, UK, 1973; pp. 245–249.
49. Anselin, L. Local indicators of spatial association—LISA. *Geogr. Anal.* **1995**, *27*, 93–115. [CrossRef]
50. Anselin, L.; Syabri, I.; Kho, Y. GeoDa: An introduction to spatial data analysis. In *Handbook of Applied Spatial Analysis: Software Tools, Methods and Applications*; Springer: Berlin/Heidelberg, Germany, 2009; pp. 73–89.
51. Pontius, R.G.; Shusas, E.; McEachern, M. Detecting important categorical land changes while accounting for persistence. *Agric. Ecosyst. Environ.* **2004**, *101*, 251–268. [CrossRef]

52. Belzile, F.; Labbé, J.; LeBlanc, M.-C.; Lavoie, C. Seeds contribute strongly to the spread of the invasive genotype of the common reed (*Phragmites australis*). *Biol. Invasions* **2010**, *12*, 2243–2250. [CrossRef]
53. Kirk, H.; Paul, J.; Straka, J.; Freeland, J.R. Long-distance dispersal and high genetic diversity are implicated in the invasive spread of the common reed, *Phragmites australis* (Poaceae), in northeastern North America. *Am. J. Bot.* **2011**, *98*, 1180–1190. [CrossRef]
54. Brodersen, C.; Lavergne, S.; Molofsky, J. Genetic variation in photosynthetic characteristics among invasive and native populations of reed canarygrass (*Phalaris arundinacea*). *Biol. Invasions* **2008**, *10*, 1317–1325. [CrossRef]
55. Nan, D.; Yu-xin, T.; Qing-an, S. Characteristicso of microbial structure of typical plant comminities in south dongting lake poplar clearing area. *J. Ecol. Rural Environ.* **2022**, *38*, 915–924. [CrossRef]
56. An, X.; Zhang, M.; Zang, Z. Driving Mechanisms of Spatiotemporal Heterogeneity of Land Use Conflicts and Simulation under Multiple Scenarios in Dongting Lake Area. *Remote Sens.* **2023**, *15*, 4524. [CrossRef]
57. Décamps, H. The renewal of floodplain forests along rivers: A landscape perspective. *Int. Ver. Für Theor. Und Angew. Limnol. Verhandlungen* **1996**, *26*, 35–59. [CrossRef]
58. Fischer, M.; Trnka, M.; Kučera, J.; Deckmyn, G.; Orság, M.; Sedlák, P.; Žalud, Z.; Ceulemans, R. Evapotranspiration of a high-density poplar stand in comparison with a reference grass cover in the Czech–Moravian Highlands. *Agric. For. Meteorol.* **2013**, *181*, 43–60. [CrossRef]
59. Hu, W.; Li, G.; Li, Z. Spatial and temporal evolution characteristics of the water conservation function and its driving factors in regional lake wetlands—Two types of homogeneous lakes as examples. *Ecol. Indic.* **2021**, *130*, 108069. [CrossRef]
60. Mao, B.; Wang, X.; Liao, Z.; Miao, Y.; Yan, S. Spatiotemporal variations and tradeoff-synergy relations of ecosystem services under ecological water replenishment in Baiyangdian Lake, North China. *J. Environ. Manag.* **2023**, *343*, 118229. [CrossRef] [PubMed]
61. Hongwang, L.; Wenmin, H.; Jiyun, S.; Wen, Z.; Yabin, S. Study on the influence of Ecological Poplar Withdrawal on the landscape pattern of Dongting Lake wetland. *J. Nanjing For. Univ.* **2020**, *44*, 171–178.
62. Kamocki, A.K.; Kołos, A.; Banaszuk, P. Can we effectively stop the expansion of trees on wetlands? Results of a birch removal experiment. *Wetl. Ecol. Manag.* **2017**, *25*, 359–367. [CrossRef]
63. Zhang, P.; Zou, Y.; Xie, Y.; Zhang, H.; Liu, X.; Gao, D.; Yi, F. Shifts in distribution of herbivorous geese relative to hydrological variation in East Dongting Lake wetland, China. *Sci. Total Environ.* **2018**, *636*, 30–38. [CrossRef]
64. Liu, Y.; Shi, L.; Duo, H.; Peng, B.; Lü, C.; Zhu, Y.; Lei, G. Disturbance-driven changes to landscape patterns and responses of waterbirds at West Dongting Lake, China. *Biodivers. Sci.* **2013**, *21*, 666–676.
65. Luo, K.; Wu, Z.; Bai, H.; Wang, Z. Bird diversity and waterbird habitat preferences in relation to wetland restoration at Dianchi Lake, south-west China. *Avian Res.* **2019**, *10*, 21. [CrossRef]
66. Yuan, L.; Liu, D.; Tian, B.; Yuan, X.; Bo, S.; Ma, Q.; Wu, W.; Zhao, Z.; Zhang, L.; Keesing, J.K. A solution for restoration of critical wetlands and waterbird habitats in coastal deltaic systems. *J. Environ. Manag.* **2022**, *302*, 113996. [CrossRef]
67. Qu, X.; Du, C.; Wu, H.; Xiong, Y.; Yu, G.; Wang, J.; Dai, J.; Wu, L.; Zhang, Z.; Zhu, Y.; et al. Effects of Poplar Ecological Retreat on Habitat Suitability for Migratory Birds in China's Dongting Lake Wetland. *Front. Environ. Sci.* **2022**, *9*, 793005. [CrossRef]
68. Yue, T.; Yonghong, X.; Feng, L. Spatial distribution of emergent herbaceous wetlands in the east dongting lake during the last twenty years based on Landsat data. *Resour. Environ. Yangtze Basin* **2013**, *22*, 1484–1492.
69. Wang, T.; Deng, Z.; Zhang, C.; Zou, Y.; Xie, Y.; Li, F.; Xiao, F.; Peng, C. Vegetation types and flood water level are dominant factors controlling the carbon sequestration potential in Dongting Lake floodplain, China. *Sci. Total Environ.* **2024**, *921*, 171146. [CrossRef]
70. Hohman, T.R.; Howe, R.W.; Tozer, D.C.; Giese, E.E.G.; Wolf, A.T.; Niemi, G.J.; Gehring, T.M.; Grabas, G.P.; Norment, C.J. Influence of lake levels on water extent, interspersion, and marsh birds in Great Lakes coastal wetlands. *J. Great Lakes Res.* **2021**, *47*, 534–545. [CrossRef]
71. Zhu, Y.; Wang, H.; Guo, W. The impacts of water level fluctuations of East Dongting Lake on habitat suitability of migratory birds. *Ecol. Indic.* **2021**, *132*, 108277. [CrossRef]
72. Wu, H.; Dai, J.; Sun, S.; Du, C.; Long, Y.; Chen, H.; Yu, G.; Ye, S.; Chen, J. Responses of habitat suitability for migratory birds to increased water level during middle of dry season in the two largest freshwater lake wetlands of China. *Ecol. Indic.* **2021**, *121*, 107065. [CrossRef]
73. Duoduo, F.; Lei, G.; Linlu, S.; Qing, Z. Impact of Autumn Hydrologic Regime on Plants in Beach and Distribution of Population of Wintering Lesser White-fronted Goose in East Dongting Lake. *Wetl. Sci.* **2014**, *12*, 491–498. [CrossRef]
74. Mazurczyk, T.; Brooks, R.P. Carbon storage dynamics of temperate freshwater wetlands in Pennsylvania. *Wetl. Ecol. Manag.* **2018**, *26*, 893–914. [CrossRef]
75. Qi, Q.; Zhang, D.; Tong, S.; Zhang, M.; Wang, X.; An, Y.; Lu, X. The driving mechanisms for community expansion in a restored Carex tussock wetland. *Ecol. Indic.* **2021**, *121*, 107040. [CrossRef]
76. Xi, Y.; Peng, S.; Liu, G.; Ducharne, A.; Ciais, P.; Prigent, C.; Li, X.; Tang, X. Trade-off between tree planting and wetland conservation in China. *Nat. Commun.* **2022**, *13*, 1967. [CrossRef]
77. Wu, L.; Sun, C.; Fan, F. Estimating the Characteristic Spatiotemporal Variation in Habitat Quality Using the InVEST Model—A Case Study from Guangdong–Hong Kong–Macao Greater Bay Area. *Remote Sens.* **2021**, *13*, 1008. [CrossRef]

Disclaimer/Publisher's Note: The statements, opinions and data contained in all publications are solely those of the individual author(s) and contributor(s) and not of MDPI and/or the editor(s). MDPI and/or the editor(s) disclaim responsibility for any injury to people or property resulting from any ideas, methods, instructions or products referred to in the content.